

FINITE T MESON CORRELATIONS AND QUARK DECONFINEMENT *

D. BLASCHKE † G. BURAU

*Fachbereich Physik, Universität Rostock, Universitätsplatz 1
D-18051 Rostock, Germany*

YU.L. KALINOVSKY

*Laboratory for Computing Techniques and Automation, Joint Institute for Nuclear Research
141980 Dubna, Russia*

P. MARIS, P.C. TANDY

*Center for Nuclear Research, Department of Physics, Kent State University
Kent, OH 44242, USA*

Received (received date)

Revised (revised date)

Finite temperature spatial $\bar{q}q$ correlation modes in the π and ρ channels are studied with the rainbow-ladder truncated quark Dyson-Schwinger equation and Bethe-Salpeter equation in the Matsubara formalism. To retain the finite range of the effective interaction while facilitating summation over fermion Matsubara modes necessary to ensure continuity at $T = 0$, a separable kernel is used. The model is fixed by $T = 0$ properties and it implements dynamical chiral symmetry breaking and quark confinement. Above and below the deconfinement and chiral restoration transitions, we study $M_\pi(T)$, $f_\pi(T)$ and the 3-space transverse and longitudinal masses $M_\rho^T(T)$ and $M_\rho^L(T)$. For the ρ mode we also study the strong and electromagnetic partial widths to determine the T -dependence that is generated by the quark content. The $\rho \rightarrow \pi\pi$ width decreases sharply just above the chiral restoration transition leaving the ρ with only its narrow e^+e^- width. We discuss improvements needed by this model, especially in regard to the high T behavior of the masses where we compare to lattice QCD simulations.

PACS numbers: 11.10.St, 11.10.Wx, 12.38.Mh, 14.40.-n, 24.85.+p

1. Introduction

The connection between hot dense hadronic matter and a plasma of quarks and gluons is receiving increased attention with the advent of the relativistic heavy-ion collider (RHIC) at Brookhaven to complement previous investigations at the CERN SPS ¹. The plasma is expected to reveal itself through modified properties of hadronic reactions and their products. The di-lepton spectra has been of considerable interest ² as a relatively clean signal of how vector meson correlations and their decay channels and widths might be influenced by a hot and dense environment. The question of how a vector meson strong decay, such as $\rho \rightarrow \pi\pi$, might respond as the temperature T or chemical potential μ crosses the critical phase

*Supported by DAAD and NSF under Grant Nos. INT96-03385 and PHY97-22429.

†E-mail address: david.blaschke@physik.uni-rostock.de

boundary for chiral restoration or quark deconfinement requires that this process be studied at the quark-gluon level. To this end it is desirable to be able to describe quark deconfinement and chiral restoration at finite T and μ in a manner that can be extended to a variety of hadronic observables in a rapid and transparent way. The present model provides a simple framework for such investigations.

At $T = \mu = 0$ significant progress has been made within a continuum approach to modeling non-perturbative QCD based on the truncated Dyson-Schwinger equations (DSEs) ^{3,4,5}. An attractive feature of this approach is that dynamical chiral symmetry breaking and quark confinement can be embodied in the infrared structure of the dressed gluon 2-point function which is constrained by a few chiral meson observables. Recent works have employed the ladder-rainbow truncation of the coupled quark DSE and $\bar{q}q$ Bethe-Salpeter equation (BSE) to produce successful descriptions of masses and decay constants of the light pseudoscalars π and K ⁶ and the vectors ρ , ϕ , and K^* ⁷. These works have incorporated the one-loop renormalization group evolution of scale characteristic of QCD. With a few exceptions ⁸, applications to other hadron observables, including electromagnetic form factors and coupling constants such as $g_{\rho\pi\pi}$, have usually required the use of simpler models ^{9,10,11,12}.

The finite T, μ extension of realistic DSE/BSE models receives extra complications due to the breaking of $O(4)$ symmetry and the dynamical coupling between Matsubara modes ^{4,13,14}. These difficulties are compounded in the subsequent generation of hadronic observables via straightforward adaptation of the approach ⁹ found to be successful at $T = \mu = 0$. Studies of hadronic observables at finite T, μ in DSE/BSE models have been restricted to simplifications such as extensions of the infrared-dominant (ID) model ¹⁵ in which the effective gluon propagator is restricted to an integrable singularity at zero momentum. Nevertheless such a model has proved capable of yielding qualitatively useful information ^{16,17,18}.

In this work we explore a separable Ansatz that can implement the essential qualitative features of DSE/BSE models at finite temperature. Separable representations have previously been found capable of an efficient modeling of the effective $\bar{q}q$ interaction in the infrared domain for $T = 0$ meson observables ^{19,20}. A previous implementation at $T > 0$ employed an instantaneous separable interaction without a quark confinement mechanism ²¹. Here the approach is covariant and the simple separable interaction absolutely confines quarks at $T = 0$. The few parameters are fixed by π and ρ/ω properties. The approach is a simplification of one developed earlier ²⁰ that was found to be quite successful for the light meson spectrum at $T = 0$. The confining mechanism is an infrared enhancement in the quark-quark interaction that is strong enough to remove the possibility of a mass shell pole in the quark propagator for real p^2 . In the simple implementation used here, it is particularly transparent that sufficiently high temperature will necessarily restore a quark mass-shell pole and there will be a deconfinement transition. This model also implements low temperature dynamical chiral symmetry breaking and it preserves the Goldstone theorem in that the generated π is massless in the chiral limit. The

solutions of the BSE for the π and ρ modes are particularly simple and are used to study the T -dependence of the meson masses and decay constants in the presence of both deconfinement and chiral restoration mechanisms. Some preliminary results have been previously discussed for $T > 0$ ²² and for $T, \mu > 0$ ²³.

In Sec. II the $T = 0$ separable model is introduced, the DSE solutions for the dressed quark propagator are developed and the quark confinement property is described. The BSE solutions for π and ρ are also treated there and the corresponding decay constants are defined. The extension to $T > 0$ is considered in Sec. III and the chiral symmetry restoration and deconfinement phenomena are discussed. The spatial π and ρ modes are considered there. The Gell-Mann–Oakes–Renner (GMOR) relation and its generalization are used to evaluate the performance of this model in respecting chiral symmetry constraints. The widths of the transverse ρ from $\rho \rightarrow e^+e^-$ and $\rho \rightarrow \pi\pi$ are also considered in Sec. III. The high T behavior of the model is considered in Sec. IV by comparison of masses with results from lattice simulations. A discussion follows in Sec. V. An Appendix details the high T behavior of the ID model as a reference.

2. Confining separable Dyson-Schwinger equation model

Mesons can be described as $q\bar{q}$ bound states using the Bethe-Salpeter equation. In the ladder truncation, this equation reads[‡]

$$-\lambda(P^2)\Gamma(p, P) = \frac{4}{3} \int \frac{d^4q}{(2\pi)^4} D_{\mu\nu}^{\text{eff}}(p-q)\gamma_\mu S(q_+) \Gamma(q, P) S(q_-)\gamma_\nu, \quad (1)$$

where P is the total momentum, $q_\pm = q \pm P/2$, and $D_{\mu\nu}^{\text{eff}}(k)$ an “effective gluon propagator”. The meson mass is identified from $\lambda(P^2 = -M^2) = 1$. In conjunction with the rainbow truncation for the quark DSE

$$S(p)^{-1} = Z_2 i\gamma \cdot p + Z_2 m_0 + \frac{4}{3} \int \frac{d^4q}{(2\pi)^4} g^2 D_{\mu\nu}^{\text{eff}}(p-q)\gamma_\mu S(q)\gamma_\nu. \quad (2)$$

this equation forms the basis for the DSE approach to meson physics ^{3,4}.

Recent studies have employed $D_{\mu\nu}^{\text{eff}}(k) = \mathcal{G}(k^2)D_{\mu\nu}^{\text{free}}(k)$ where $D_{\mu\nu}^{\text{free}}(k)$ is the free gluon propagator in Landau gauge. The effective coupling $\mathcal{G}(k^2)$ is given by the one-loop perturbative form of the QCD running coupling in the ultraviolet while the phenomenological infrared form is chosen to reproduce the pion and kaon masses and decay constants ⁶. This model can successfully describe the vector meson masses and dominant decays ⁷, as well as the pion and kaon electromagnetic form factors ⁸, without new parameters.

The direct extension of such an approach to accommodate finite temperature ²⁵ and baryon density entails a significant increase in complexity. In the Matsubara formalism, the number of coupled equations represented by Eqs. (1) and (2) scales up with the number of fermion Matsubara modes included. For studies near and

[‡]We use a Euclidean space formulation, with $\{\gamma_\mu, \gamma_\nu\} = 2\delta_{\mu\nu}$, $\gamma_\mu^\dagger = \gamma_\mu$ and $a \cdot b = \sum_{i=1}^4 a_i b_i$.

above the transition, $T \geq 100$ MeV, about 10 such modes appear adequate²⁵. The appropriate number can be $\sim 10^3$ if reasonable continuity with $T = 0$ results is to be verified. Meson $\bar{q}q$ modes at $T > 0$ have often been studied within the Nambu–Jona-Lasinio model where the contact nature of the effective interaction allows decoupling of the Matsubara modes and also analytic methods of summation, see for example, Ref.²⁶ and references therein. However the lack of quark confinement in that model leads to unphysical thresholds for $\bar{q}q$ dissociation.

We consider here a simple separable interaction that has a finite range, accommodates quark confinement, and facilitates a decoupling of fermion Matsubara modes. We base our approach on a confining separable model²⁰ previously found to be successful at $T = 0$ and defined by $D_{\mu\nu}^{\text{eff}}(p - q) \rightarrow \delta_{\mu\nu} D(p^2, q^2, p \cdot q)$ with

$$D(p^2, q^2, p \cdot q) = D_0 f_0(p^2)f_0(q^2) + D_1 f_1(p^2)(p \cdot q)f_1(q^2). \quad (3)$$

Here a Feynman-like gauge is chosen for phenomenological simplicity. This is a rank-2 interaction with two strength parameters D_0, D_1 , and corresponding form factors $f_i(p^2)$. The choice for these quantities is constrained by consideration of the resulting solution of the DSE for the quark propagator in the rainbow approximation. For the amplitudes defined by $S(p) = [i\not{p}A(p^2) + B(p^2) + m_0]^{-1}$ this produces[§]

$$B(p^2) = \frac{16}{3} \int \frac{d^4q}{(2\pi)^4} D(p^2, q^2, p \cdot q) \frac{B(q^2) + m_0}{q^2 A^2(q^2) + [B(q^2) + m_0]^2}, \quad (4)$$

$$[A(p^2) - 1] p^2 = \frac{8}{3} \int \frac{d^4q}{(2\pi)^4} D(p^2, q^2, p \cdot q) \frac{(p \cdot q)A(q^2)}{q^2 A^2(q^2) + [B(q^2) + m_0]^2}. \quad (5)$$

We note that if terms of higher order in $p \cdot q$ were to be included in Eq. (3), they would make no contribution to Eqs. (4) and (5) for the DSE solution²⁰. The solution for $B(p^2)$ is determined only by the D_0 term, and the solution for $A(p^2) - 1$ is determined only by the D_1 term. Eq. (3) produces solutions having the form

$$B(p^2) = b f_0(p^2), \quad A(p^2) = 1 + a f_1(p^2), \quad (6)$$

and Eqs. (4) and (5) reduce to nonlinear equations for the constants b and a .

2.1. Confinement and Dynamical Chiral Symmetry Breaking

If there are no poles in the quark propagator $S(p)$ for real timelike p^2 then there is no physical quark mass shell, quarks cannot propagate free of interactions, and the description of hadronic processes will not be hindered by spurious quark production thresholds. This is sufficient but not necessary for quark confinement and it remains a viable possibility for how quark confinement is realized^{27,28}. The more general phenomena of confinement of colored multi-quark states and the non-existence of S-matrix elements connecting them to hadronic states are more subtle topics that

[§]We choose the interaction form factors such that they provide sufficient ultraviolet suppression. Therefore no renormalization is needed and $Z_2 = 1$.

do not concern us here³. A nontrivial solution for $B(p^2)$ in the chiral limit ($m_0 = 0$) signals dynamical chiral symmetry breaking. There is a connection between quark confinement as the lack of a quark mass shell and the existence of a strong quark mass function in the infrared through dynamical chiral symmetry breaking. This connection has proved to be empirically successful for the description of ground state light quark mesons and their form factors and decays^{9,11}. In the present separable model the strength $b = B(0)$, which is generated by solution of Eqs. (4) and (5), controls both confinement and dynamical chiral symmetry breaking.

The propagator is confining if $m^2(p^2) \neq -p^2$ for real p^2 where the quark mass function is $m(p^2) = (B(p^2) + m_0)/A(p^2)$. With an exponential form factor $f_0(p^2) = \exp(-p^2/\Lambda_0^2)$, this condition is most transparent in the case of a rank-1 separable model where $D_1 = 0$ and $A(p^2) = 1$, i.e., $a = 0$. In the chiral limit, the model is confining if D_0 is strong enough to make $b/\Lambda_0 \geq 1/\sqrt{2e}$ and this finite b also signals dynamical chiral symmetry breaking. Using $\Lambda_0 \sim 0.6 - 0.8$ GeV as a typical range for a quark mass function $m(p^2)$, both confinement and dynamical chiral symmetry breaking will be compatible with $m(p=0) \geq 0.3$ GeV, an empirically viable value. The above qualitative properties will also hold in the case of a rank-2 model if the form factor ranges satisfy $\Lambda_1 > \Lambda_0$ and this is compatible with empirical findings that the amplitude $A(p^2)$ typically has a larger momentum range than $B(p^2)$. At finite temperature, the strength $b(T)$ for the quark mass function will decrease with T so that this model can be expected to have a deconfinement transition at or before the chiral restoration transition associated with $b(T) \rightarrow 0$.

It is found that the simple choice $f_i(p^2) = \exp(-p^2/\Lambda_i^2)$ produces numerical solutions that describe infrared properties of π and ω mesons very well and generate an empirically acceptable chiral condensate. At the same time the produced quark propagator is found to be confining and the infrared strength and shape of the quark amplitudes $A(p^2)$ and $B(p^2)$ are in qualitative agreement with the results of typical DSE studies⁶. We use the exponential form factors as a minimal way to preserve these properties while realizing that the ultraviolet suppression is much greater than the power law fall-off (with logarithmic corrections) known from asymptotic QCD. Most of our investigation centers on physics below and in the vicinity of the transition. We use the high T behavior of masses in comparison with lattice results to discuss improvements appropriate for future work.

2.2. π and ρ bound states

With the separable interaction of Eq. (3), the allowed form of the solution of Eq. (1) for the pion BS amplitude $\vec{\tau}\Gamma_\pi(q; P)$ is²⁰

$$\Gamma_\pi(q; P) = \gamma_5 (iE_\pi(P^2) + \not{P}F_\pi(P^2)) f_0(q^2), \quad (7)$$

which contains the two dominant covariants from the set of four general covariants. The q dependence is described only by the first form factor $f_0(q^2)$. The second term f_1 of the interaction can contribute only indirectly via the quark propagators. The π BSE, Eq. (1), becomes a 2×2 matrix eigenvalue problem $\mathcal{K}(P^2)f = \lambda(P^2)f$

where the eigenvector is $f = (E_\pi, F_\pi)$. The kernel is

$$\mathcal{K}_{ij}(P^2) = -\frac{4D_0}{3} \text{tr}_s \int \frac{d^4q}{(2\pi)^4} f_0^2(q^2) [\hat{t}_i S(q_+) t_j S(q_-)] , \quad (8)$$

where the π covariants are $t = (i\gamma_5, \gamma_5 \not{P})$ and we have also introduced $\hat{t} = (i\gamma_5, -\gamma_5 \not{P}/2P^2)$. We note that the separable model produces the same q^2 shape for both amplitudes F_π and E_π ; the shape is that of the quark amplitude $B(q^2)$. For the general amplitude $E_\pi(q; P)$ this is the correct shape in the chiral limit; for physical quark masses it is still a very good approximation⁶. In general, the amplitude $F_\pi(q; P)$ does not have that shape; it is in fact linked with $A(q^2) - 1$ through the axial vector Ward-Takahashi identity (AV-WTI)²⁹. However Goldstone's theorem, the key consequence of the AV-WTI, is preserved by the present separable model; in the chiral limit, whenever a nontrivial DSE solution for $B(p^2)$ exists, there will be a massless π solution to Eq. (8).

A simple illustrative truncation is obtained by setting $F_\pi(P^2) = 0$ for then Eq. (8) reduces to an expression for the eigenvalue which is

$$\lambda_\pi(P^2) = \frac{16D_0}{3} \int \frac{d^4q}{(2\pi)^4} f_0^2(q^2) \left[\left(q^2 - \frac{P^2}{4} \right) \sigma_V^+ \sigma_V^- + \sigma_S^+ \sigma_S^- \right] , \quad (9)$$

where the quark propagator amplitudes employed here are defined by $S(p) = -i\not{p} \sigma_V(p^2) + \sigma_S(p^2)$. Since $A = 1$ in rank-1, we omit the amplitude F_π in that case. Thus it is Eq. (9) that we use for the π calculation with a rank-1 interaction.

The vector mesons ρ and ω are degenerate in the ladder approximation. We shall deal with the isovector ρ . For the BS amplitude $\vec{\tau} \Gamma_\mu^\rho(q; P)$ there are in general eight transverse covariants⁷ and the dominant one is $\gamma_\mu^T(P) = T_{\mu\nu}(P) \gamma_\nu$ where $T_{\mu\nu}(P) = \delta_{\mu\nu} - P_\mu P_\nu / P^2$. The solution of the rank-1 model contains only that term, that is, $\Gamma_\mu^\rho(q; P) = \gamma_\mu^T(P) f_0(q^2) F_\rho(P^2)$. The corresponding eigenvalue is given by

$$\lambda_\rho(P^2) = \frac{8D_0}{3} \int \frac{d^4q}{(2\pi)^4} f_0^2(q^2) \left[\left(q^2 - \frac{P^2}{4} - \frac{2q^2}{3}(1-z^2) \right) \sigma_V^+ \sigma_V^- + \sigma_S^+ \sigma_S^- \right] , \quad (10)$$

where $z = \hat{q} \cdot \hat{P}$. For the rank-2 separable interaction, there are two other covariants besides γ_μ^T that will appear in the solution of the BSE²⁰. However it has been found in such a model that these subleading vector covariants make only a few percent contribution to the vector mass²⁰ and the associated $g_{\rho\pi\pi}$ ¹¹. In this present work we will ignore the subdominant covariants and employ γ_μ^T as the only covariant for the vector meson. The differences in the vector mass obtained from Eq. (10) in rank-1 and rank-2 will be due to differences in the quark propagator in each case.

The normalization condition for the π BS amplitude can be expressed as

$$2P_\mu = \frac{\partial}{\partial P_\mu} 2N_c \text{tr}_s \int \frac{d^4q}{(2\pi)^4} \bar{\Gamma}_\pi(q; -K) S(q_+) \Gamma_\pi(q; K) S(q_-) \Big|_{P^2=K^2=-M_\pi^2} . \quad (11)$$

Here $\bar{\Gamma}(q; K)$ is the charge conjugate amplitude $[\mathcal{C}^{-1}\Gamma(-q, K)\mathcal{C}]^t$ where $\mathcal{C} = \gamma_2\gamma_4$ and t denotes matrix transpose. This defines a normalization constant N_π via $E_\pi(P^2 = -M_\pi^2) f_0(q^2) = B(q^2)/N_\pi$. The pion decay constant f_π can be expressed as the loop integral

$$\begin{aligned} f_\pi P_\mu \delta_{ij} &= \langle 0 | \bar{q} \frac{\tau_i}{2} \gamma_\mu \gamma_5 q | \pi_j(P) \rangle \\ &= \delta_{ij} N_c \text{tr}_s \int \frac{d^4 q}{(2\pi)^4} \gamma_5 \gamma_\mu S(q_+) \Gamma_\pi(q; P) S(q_-). \end{aligned} \quad (12)$$

Note that Eq. (12) is the exact expression for f_π except for the absence of the renormalization constant Z_2 which is unity in the present model. The decay constants thus test the quality of the infrared behavior of the quark propagator and the BS amplitudes. Similar expressions exist for the normalization of the vector meson BS amplitude and the coupling between a vector meson and a photon ^{7,12}.

Table 1. Calculated properties at $T = 0$ for the u/d quark mesons π and ρ along with related quark properties and parameters for the rank-1 and rank-2 separable models. The quoted experimental values for both the quark condensate and the current u/d quark mass m_0 are appropriate to a renormalization scale of $\mu \sim 1$ GeV. The scale for the model calculations may be considered to be set by Λ_0 .

	Experiment	rank-1	rank-2
$-\langle \bar{q}q \rangle^0$	$(0.236 \text{ GeV})^3$	0.248	0.203
m_0	5 - 10 MeV	6.6	5.3
$m(p^2 = 0)$	~ 0.350 GeV	0.685	0.405
M_π	0.1385 GeV	0.140	0.139
f_π	0.093 GeV	0.104	0.093
N_π/f_π	1.0	0.987	0.740
M_ρ/ω	0.770/0.783 GeV	0.783	0.784
g_ρ	5.04	5.04	6.38
$\Gamma_{\rho^0 \rightarrow e^+ e^-}$	6.77 keV	6.76	4.22
$g_{\rho\pi\pi}$	6.05	5.71	7.22
$\Gamma_{\rho \rightarrow \pi\pi}$	151 MeV	137	221
Parameters			
$D_0 \Lambda_0^2$		128.0	260.0
Λ_0		0.687 GeV	0.638 GeV
$D_1 \Lambda_1^4$		0	130.0
Λ_1/Λ_0			1.21

In Table 1 the results for the ground state π and ρ/ω mesons as well as related quantities are shown for both rank-1 and rank-2 versions of the model along with the values of the employed parameters. We consider the experimental ω mass to be the appropriate value for comparison with the vector result in ladder approximation in order to allow for subsequent preferential lowering of M_ρ due to pion loop dressing ³⁰. The range parameter Λ_0 is used to set the mass scale to reproduce the experimental M_ω for rank-1 and f_π for rank-2. The obtained dynamical quark mass function at $p^2 = 0$ is $m(p^2 = 0) = 0.685$ GeV for rank-1. For rank-2 we obtain $A(p^2 = 0) = 1.94$ and $m(p^2 = 0) = 0.405$ GeV. In both cases the dressed quark propagator is confining. The strengths obtained for the mass function are consistent with results from recent DSE solutions ^{6,7}. Also shown in Table 1 are

the results obtained for the electromagnetic (g_ρ) and strong decays ($g_{\rho\pi\pi}$) of the ρ , which compare reasonably well with experiments.

The difference between N_π and f_π shown in Table 1 simply reflects the fact that the AV-WTI cannot be exactly satisfied within a separable model. (This is also the case in the Nambu–Jona-Lasinio model due to the required cut-off and in any approach that does not use a translationally invariant interaction or a sufficiently complete set of Dirac covariants for Γ_π and the vertex amplitudes²⁹.) A translationally invariant model that makes the simplifying assumption $A(p^2) = 1$ can achieve a fortuitous agreement³ and this dominates the rank-1 result for N_π/f_π . Rather than use f_π to define N_π , we calculate N_π from its definition in Eq. (11) so that, in subsequent studies of processes such as $\rho \rightarrow \pi\pi$, the pion state is physically and consistently normed within the model.

3. Finite Temperature Extension

The extension of the separable model studies to $T \neq 0$ is systematically accomplished by transcription of the Euclidean quark 4-momentum via $q \rightarrow q_n = (\omega_n, \vec{q})$, where $\omega_n = (2n + 1)\pi T$ are the discrete Matsubara frequencies. The effective $\bar{q}q$ interaction will automatically decrease with increasing T without the introduction of an explicit T -dependence which would require new parameters. We investigate the resulting behavior of the π and ρ meson modes and decays in the presence of deconfinement and chiral restoration.

3.1. Chiral symmetry restoration and deconfinement

The result of the DSE solution for the dressed quark propagator now becomes

$$S^{-1}(p_n, T) = i\vec{\gamma} \cdot \vec{p} A(p_n^2, T) + i\gamma_4 \omega_n C(p_n^2, T) + B(p_n^2, T) + m_0, \quad (13)$$

where $p_n^2 = \omega_n^2 + \vec{p}^2$ and there are now three amplitudes due to the loss of $O(4)$ symmetry. The solutions have the form $B = b(T)f_0(p_n^2)$, $A = 1 + a(T)f_1(p_n^2)$, and $C = 1 + c(T)f_1(p_n^2)$ and the DSE becomes a set of three non-linear equations for $b(T)$, $a(T)$ and $c(T)$. The explicit form is

$$a(T) = \frac{8D_1}{9} T \sum_n \int \frac{d^3p}{(2\pi)^3} f_1(p_n^2) \vec{p}^2 [1 + a(T)f_1(p_n^2)] d^{-1}(p_n^2, T), \quad (14)$$

$$c(T) = \frac{8D_1}{3} T \sum_n \int \frac{d^3p}{(2\pi)^3} f_1(p_n^2) \omega_n^2 [1 + c(T)f_1(p_n^2)] d^{-1}(p_n^2, T), \quad (15)$$

$$b(T) = \frac{16D_0}{3} T \sum_n \int \frac{d^3p}{(2\pi)^3} f_0(p_n^2) [m_0 + b(T)f_0(p_n^2)] d^{-1}(p_n^2, T), \quad (16)$$

where $d(p_n^2, T)$ is given by

$$d(p_n^2, T) = \vec{p}^2 A^2(p_n^2, T) + \omega_n^2 C^2(p_n^2, T) + [m_0 + B(p_n^2, T)]^2. \quad (17)$$

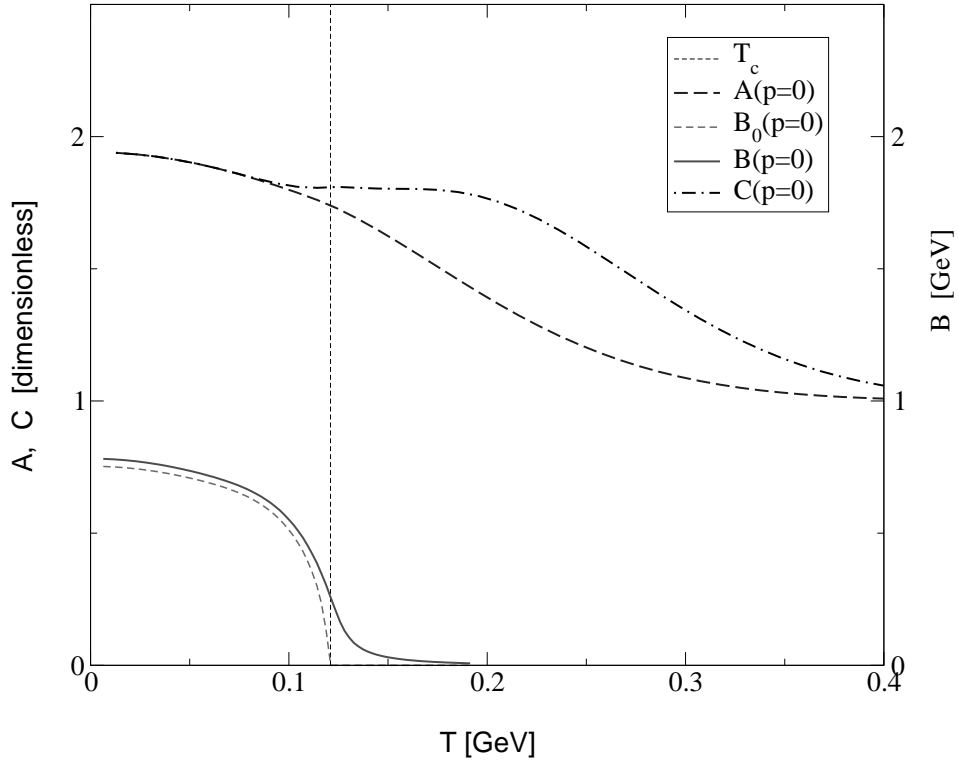


Figure 1: T -dependence of quark self-energy amplitudes at $p = 0$ from solution of the DSE.

It is also useful to introduce the equivalent representation

$$S(p_n, T) = -i\vec{\gamma} \cdot \vec{p} \sigma_A(p_n^2, T) - i\gamma_4 \omega_n \sigma_C(p_n^2, T) + \sigma_B(p_n^2, T), \quad (18)$$

where $\sigma_A = A/d$, $\sigma_C = C/d$ and $\sigma_B = (B + m_0)/d$.

The T -dependence of the solutions for A, B and C at $\vec{p}^2 = 0$ for the rank-2 model is displayed in Fig. 1. The results shown are for the lowest Matsubara mode ($n = 0$) which provides the leading behavior as T is increased. The chiral restoration critical temperature T_c is identified from the vanishing of the chiral limit amplitude $B_0(p = 0, T)$ as shown. We find $T_c = 121$ MeV for the rank-2 model. Below T_c , A and C are relatively constant, $O(4)$ symmetry is approximately manifest, and the main effect is an almost constant quark wave function renormalization via $1/C$; the central feature shared by both rank-1 and rank-2 models is a rapidly decreasing mass function. Above T_c , there remains a significant temperature range where the self-interaction effects are strong, both A and C are considerably enhanced above their perturbative values, and the breaking of $O(4)$ symmetry is manifest. The present model thus captures the qualitative T -dependence observed for the dressed quark propagator in studies of the quark DSE^{13,16}. The rank-1 limit has $A = C = 1$

for all T and the behavior of $B(p=0, T)$ is similar to that in Fig. 1 except $T_c = 146$ MeV is obtained.

The order parameter for chiral restoration, the chiral quark condensate, can be obtained from the chiral limit quark propagator as $\langle \bar{q}q \rangle^0 = -N_c \text{tr}_s S_0(x, x)$. Here this produces

$$\langle \bar{q}q \rangle^0 = -4N_c T \sum_n \int \frac{d^3p}{(2\pi)^3} \frac{b_0(T) f_0(p_n^2)}{d_0(p_n^2, T)}, \quad (19)$$

where b_0 and d_0 are obtained from the chiral limit solution of the DSE. Both $b_0(T)$ and $\langle \bar{q}q \rangle^0$ vanish sharply as $(1 - T/T_c)^\beta$ with the critical exponent having the mean field value $\beta = 1/2$ in agreement with other rainbow DSE studies³¹.

The deconfinement temperature T_d is found by a search for a propagator pole (a zero of the function $d(p_0^2, T)$) on the real \vec{p}^2 axis. We find $T_d = T_c = 146$ MeV for the rank-1 model and $T_d = 0.9 T_c = 105$ MeV for the rank-2 model. Only about 15% variation in these transition temperatures can be achieved by variation of the model parameters while retaining a reasonable description of the observables shown in Table 1. Since all dynamical information concerning the rank-1 model is contained in one function $B(p_n^2, T)$, one may expect to find $T_d = T_c$ in that case. For rank-2, the dynamical information is contained in three functions and the result $T_d \neq T_c$ is not surprising. It is however possible that the separable form of interaction used here might miss some dynamical correlations between A, B and C that would otherwise produce $T_d = T_c$.

3.2. Spatial π correlations at $T \neq 0$

At $T = 0$ the mass-shell condition for a meson as a $\bar{q}q$ bound state of the BSE is equivalent to the appearance of a pole in the $\bar{q}q$ scattering amplitude as a function of P^2 . At $T \neq 0$ in the Matsubara formalism, the $O(4)$ symmetry is broken by the heat bath and we have $P \rightarrow (\Omega_m, \vec{P})$ where $\Omega_m = 2m\pi T$. Bound states and the poles they generate in propagators may be investigated through polarization tensors, correlators or Bethe-Salpeter eigenvalues. This pole structure is characterized by information at discrete points Ω_m on the imaginary energy axis and at a continuum of 3-momenta. Analytic continuation for construction of real-time Green's functions (and related propagation properties) has been well-studied³². An unambiguous result is obtained by requiring that the continuation yield a function that is bounded at complex infinity and analytic off the real axis³². One may search for poles as a function of \vec{P}^2 thus identifying the so-called spatial or screening masses for each Matsubara mode. These serve as one particular characterization of the propagator and the $T > 0$ bound states.

In the present context the eigenvalues of the meson BSE become $\lambda(P^2) \rightarrow \tilde{\lambda}(\Omega_m^2, \vec{P}^2; T)$. The temporal meson masses identified by zeros of $1 - \tilde{\lambda}(\Omega^2, 0; T)$ will be different in general from the spatial masses identified by zeros of $1 - \tilde{\lambda}(0, \vec{P}^2; T)$. They are however identical at $T = 0$ and an approximate degeneracy can be expected to extend over the finite T domain where the $O(4)$ symmetry is not strongly broken. From Fig. 1 one may reasonably expect this domain to extend up to

$T \sim 80 - 100$ MeV. At and above the transition, temporal and spatial masses can be expected to emphasize different aspects of the bound state modes. In this work we explore the T -dependence of the lowest spatial masses in the π and ρ channels.

In the π channel, the correlator $\Pi(x) = \langle T J_{ps}(x) J_{ps}(0) \rangle$ of two currents $J_{ps}(x) = \bar{q}(x)\gamma_5 q(x)$, after transformation to momentum space and extension to $T > 0$ via the Matsubara formalism, can be expressed as

$$\Pi(\Omega^2, \vec{P}^2) = N_c T \sum_n \text{tr}_s \int \frac{d^3 q}{(2\pi)^3} \gamma_5 S(q_{n+}) \Gamma_{ps}(q_n; \Omega, \vec{P}) S(q_{n-}), \quad (20)$$

where $q_{n\pm} = q_n \pm P/2$ and Γ_{ps} is the pseudoscalar vertex which satisfies the inhomogeneous version of the pion BSE. The quark propagators appearing here are dressed according to solution of the DSE. When the ladder approximation is employed for Γ_{ps} , along with the present separable approximation to the BSE kernel, the correlation function can be expressed as

$$\Pi(\Omega^2, \vec{P}^2) = \Pi^{(0)}(\Omega^2, \vec{P}^2) - \frac{4D_0}{3} N_c L_i(\Omega^2, \vec{P}^2) [1 - \mathcal{K}(\Omega^2, \vec{P}^2)]_{ij}^{-1} \hat{L}_j(\Omega^2, \vec{P}^2). \quad (21)$$

Here $\Pi^{(0)}$ is the contribution to Eq. (20) arising from the zeroth order contribution (γ_5) to the pseudoscalar vertex Γ_{ps} . The second term of Eq. (21) sums the interaction terms and factorizes due the separability of the effective interaction. The kernel \mathcal{K} involves the $T > 0$ extension of the kernel of the π separable BSE given previously in Eq. (8). The loop integrals for the numerator are given by

$$L_i(\Omega^2, \vec{P}^2) = T \sum_n \text{tr}_s \int \frac{d^3 q}{(2\pi)^3} f_0(q_n^2) \gamma_5 S(q_{n+}) t_i S(q_{n-}), \quad (22)$$

and

$$\hat{L}_j(\Omega^2, \vec{P}^2) = T \sum_n \text{tr}_s \int \frac{d^3 q}{(2\pi)^3} f_0(q_n^2) \hat{t}_j S(q_{n+}) \gamma_5 S(q_{n-}). \quad (23)$$

With an eigenvector representation of the BSE kernel \mathcal{K} , Eq. (21) develops a denominator $1 - \tilde{\lambda}_\pi(\Omega^2, \vec{P}^2; T)$. There is a pole in the correlator associated with the spatial mode solution to the homogeneous BSE identified from

$$1 - \tilde{\lambda}_\pi(0, \vec{P}^2; T) = Z_\pi^{-1}(\vec{P}^2, T) [\vec{P}^2 + M_\pi^2(T)] = 0. \quad (24)$$

The masses so identified are spatial screening masses of the lowest mode associated with the 3-space asymptotic behavior $\Pi(x) \sim \exp(-Mx)$. The identification of spatial masses by location of a pole is equivalent, by Fourier transformation, to the method of large spatial separation of sources used in lattice QCD.

The general form of the finite T pion BS amplitude allowed by the separable model is

$$\Gamma_\pi(q_n; P_m) = \gamma_5 \left(iE_\pi(P_m^2) + \gamma_4 \Omega_m \tilde{F}_\pi(P_m^2) + \vec{\gamma} \cdot \vec{P} F_\pi(P_m^2) \right) f_0(q_n^2). \quad (25)$$

The separable BSE becomes a 3×3 matrix eigenvalue problem with a kernel that is a generalization of Eq. (8). In the limit $\Omega_m \rightarrow 0$, as is required for the spatial mode of interest here, the amplitude $\hat{F}_\pi = \Omega_m \tilde{F}_\pi$ is trivially zero. The pseudovector amplitude F_π is significantly different from zero below T_c , but decreases rapidly above the transition. In the chiral limit, it vanishes identically at and beyond the transition; above the transition, only E_π survives.

The result for the π mass is displayed in Fig. 2 for rank-2; the results for the rank-1 model are similar. In both models, $M_\pi(T)$ is seen to be only weakly T -dependent until near T_c where a sharp rise begins. These qualitative features of the response of the pion mode with T agree with the results deduced from the DSE in Ref. ¹³ and also with the more detailed study of Ref. ²⁵ using a ladder-rainbow truncation of the DSE/BSE system that preserves the one-loop renormalization group properties of QCD. Evidently the detailed character of the effective interaction in the perturbative region does not dominate at the level of the present qualitative investigation.

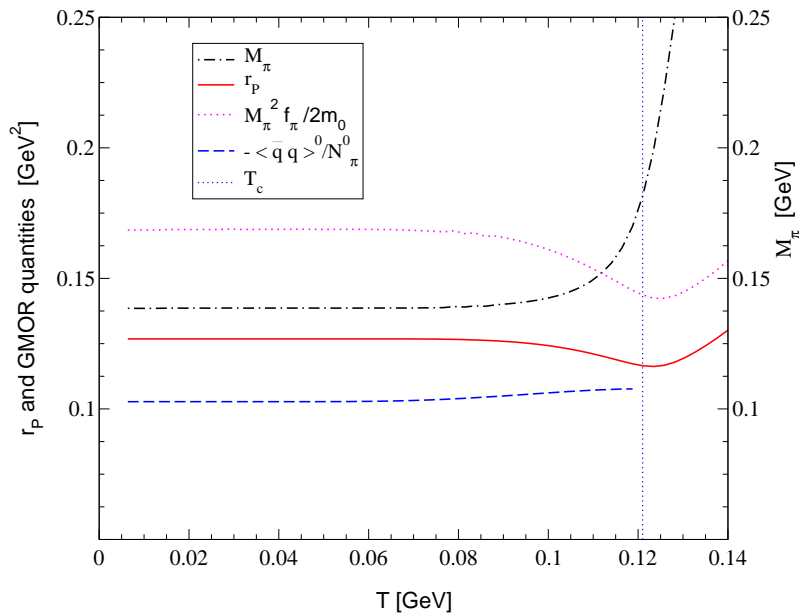


Figure 2: Chiral symmetry in the rank-2 model. T -dependence of M_π and quantities involved in the exact pion mass relation and the GMOR relation.

3.3. Chiral symmetry and π mass relation

To explore the extent to which the model respects the detailed constraints from chiral symmetry, we investigate the exact QCD pseudoscalar mass relation ²⁹ which, after extension to the spatial mode at $T > 0$, is

$$M_\pi^2(T) f_\pi(T) = 2m_0 r_P(T). \quad (26)$$

Here r_P , the residue at the pion pole in the pseudoscalar vertex, is given by the pseudoscalar projection of the pion wavefunction onto zero quark-antiquark separation, that is

$$ir_P(T) = N_c T \sum_n \text{tr}_s \int \frac{d^3q}{(2\pi)^3} \gamma_5 S(q_n + \frac{\vec{P}}{2}) \Gamma_\pi(q_n; \vec{P}) S(q_n - \frac{\vec{P}}{2}). \quad (27)$$

The generalization of Eq. (12) for f_π to finite temperature in the case of the spatial pion mode is

$$P_i f_\pi(T) = N_c T \sum_n \text{tr}_s \int \frac{d^3q}{(2\pi)^3} \gamma_5 \gamma_i S(q_n + \frac{\vec{P}}{2}) \Gamma_\pi(q_n; \vec{P}) S(q_n - \frac{\vec{P}}{2}). \quad (28)$$

Eqs. (27) and (28) are exact expressions for $r_P(T)$ and $f_\pi(T)$ except for the absence of the renormalization constants which are trivially equal to one in this separable model. The relation in Eq. (26) is a consequence of the pion pole structure of the isovector axial Ward identity which links the quark propagator, the pseudoscalar vertex and the axial vector vertex²⁹. In the chiral limit, $r_P \rightarrow -\langle \bar{q}q \rangle^0 / f_\pi^0$ and Eq.(26), for small mass, produces the Gell-Mann–Oakes–Renner (GMOR) relation. The exact mass relation, Eq. (26), can only be satisfied approximately when the various quantities are obtained in a manner that does not preserve axial Ward identity. The error can be used to assess the reliability of the present approach to modeling the behavior of the pion spatial mode as the temperature is varied.

Our findings in the case of the rank-2 model are displayed in Fig. 2. There the solid line represents $r_P(T)$ calculated from the quark loop integral in Eq. (27); the dotted line represents r_P constructed from the other quantities in Eq. (26). The exact mass relation, Eq. (26), is violated by about 25% almost independent of temperature, even above T_c . The rank-1 model satisfies this relation to within 1%, due to the special but unrealistic case $A = 1 = C$. We have also investigated the (approximate) GMOR relation within the present model. The quantity $-\langle \bar{q}q \rangle^0 / N_\pi^0$, displayed in Fig. 2, is the chiral limit of r_P in this model. If all covariants for the pion were retained and the axial vector Ward identity were obeyed, one would have $N_\pi^0 = f_\pi^0$ in the chiral limit²⁹. If the GMOR relation were exactly obeyed, the long-dashed line representing $\langle \bar{q}q \rangle^0 / N_\pi^0$ would coincide with the dotted line representing $M_\pi^2 f_\pi / 2m_0$. These features are temperature-independent until about $0.9 T_c$, consistent with an earlier study of low energy theorems at $T > 0$ within a three-space, non-confining separable interaction model³³. Close to T_c , the GMOR relation breaks down, and above T_c , it is no longer well-defined.

It should be noted that f_π^0 , N_π^0 and $\langle \bar{q}q \rangle^0$ are equivalent order parameters for the critical behavior near T_c and have weak T -dependence below T_c . A consequence is that $M_\pi^2 f_\pi$, r_P and $\langle \bar{q}q \rangle^0 / N_\pi^0$ are almost T -independent and so are the estimated errors for the two mass relations linking these quantities. We have employed the physical f_π defined at non-zero current quark mass, and this does not vanish at T_c but continuously decreases.

3.4. Spatial ρ correlations at $T \neq 0$

The $T = 0$ transverse vector meson, that we have described by the covariant γ_μ^T , splits for $T > 0$ into 3-space longitudinal and transverse modes. For the spatial modes characterized by $P = (0, \vec{P})$ the BS amplitudes are

$$\Gamma_\mu^{\rho(L)}(q_n; \vec{P}) = \delta_{\mu 4} \gamma_4 f_0(q_n^2) F_{\rho(L)}(\vec{P}^2), \quad (29)$$

and

$$\Gamma_i^{\rho(T)}(q_n; \vec{P}) = \left(\gamma_i - \frac{P_i \vec{P} \cdot \vec{\gamma}}{\vec{P}^2} \right) f_0(q_n^2) F_{\rho(T)}(\vec{P}^2). \quad (30)$$

The T -dependence of the corresponding masses is displayed in Fig. 3 for the rank-2 model. These modes are effectively degenerate and T -independent until about $T_c/2$ where the breaking of $O(4)$ invariance becomes significant. The qualitative features $M_\rho^L(T) > M_\rho^T(T)$ and $M_\rho^T(T) \approx \text{const}$ for $T < T_c$ seen here in the present context of a finite range interaction have previously been noted within the limiting case of the zero momentum range ID model¹⁷. This latter model was not applied for $T > T_c$. We discontinue the present study of the longitudinal mode at $T \sim 180$ MeV where it becomes unstable to $\bar{q}q$ dissociation. The transverse mode continues to be below the spatial $\bar{q}q$ threshold for the temperature range displayed.

The $T = 0$ expression^{7,12} for the electromagnetic coupling constant g_ρ has a straightforward extension to $T > 0$ for a transverse spatial ρ^0 mode. Use of the $\Omega_m = 0$ solution described above yields

$$\frac{M_\rho^T(T)^2}{g_\rho(T)} = \frac{N_c T}{2} \sum_n \text{tr}_s \int \frac{d^3 q}{(2\pi)^3} \gamma_i S(q_n + \frac{\vec{P}}{2}) \Gamma_i^{\rho(T)}(q_n; \vec{P}) S(q_n - \frac{\vec{P}}{2}). \quad (31)$$

With summation over enough Matsubara modes for convergence, the produced $g_\rho(T)$ tends smoothly to the previously determined $T = 0$ result. The result over a temperature range that extends just beyond T_c is displayed in Fig. 4. There it is confirmed that there is very little T -dependence below about $0.9 T_c$ where there is approximate $O(4)$ symmetry as evident in the quark propagator behavior in Fig. 1.

The impulse approximation for the $\rho\pi\pi$ vertex^{9,11}, after extension to $T > 0$ for spatial modes characterized by $Q = (0, \vec{Q})$ for the ρ and $P = (0, \vec{P})$ for the relative $\pi\pi$ momentum, takes the form

$$\begin{aligned} \Lambda_\nu(P, Q) &= P_\nu g_{\rho\pi\pi}(T) \\ &= -2N_c T \sum_n \text{tr}_s \int \frac{d^3 q}{(2\pi)^3} \Gamma_\pi(k_{n+}; -\vec{P}_+) S(q_{n+-}) \Gamma_\nu^{\rho(T/L)}(q_{n+}; \vec{Q}) \\ &\quad \times S(q_{n++}) \Gamma_\pi(k_{n-}; \vec{P}_-) S(q_{n-}). \end{aligned} \quad (32)$$

Use of Eq. (29) immediately shows that the longitudinal ρ mode cannot couple to $\pi\pi$. The temperature dependence obtained for the transverse ρ coupling constant

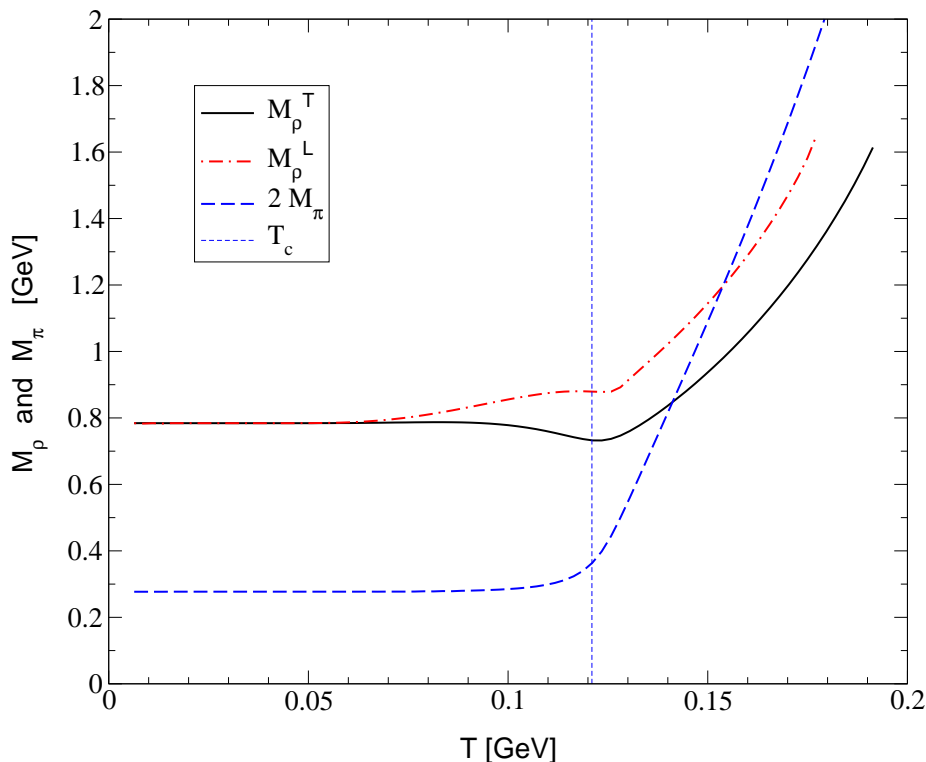


Figure 3: T -dependence of the longitudinal ρ mass (dot-dashed line) and the transverse ρ mass (solid line). Also shown is $2M_\pi$ indicating that the strong decay channel becomes inaccessible within 20-30 MeV beyond T_c . Results are from the rank-2 model.

$g_{\rho\pi\pi}(T)$ is displayed in Fig. 4. Again one observes continuity with the $T = 0$ result and a very weak T -dependence until about $0.8T_c$. Around T_c , the coupling constant decreases significantly.

For both interactions of the ρ mode, and below T_c , one expects qualitatively similar behavior from spatial modes associated with higher meson Matsubara frequencies $\Omega_m \neq 0$ except that the effect of $O(4)$ symmetry breaking will be evident earlier. Above T_c , each $2\pi T$ increment to the meson Matsubara frequency adds significantly to the quark effective mass in integrals like Eq. (31). Since dynamical chiral symmetry breaking is now absent, the quark propagators are of Dirac vector character, the meson Matsubara frequencies are the largest mass scale in the system, and perturbative behavior becomes increasingly dominant. The various spatial modes from $\Omega_m \neq 0$ are characterized by masses much greater than that of the lowest mode considered here. We anticipate that this lowest mode characterizes the qualitative behavior of the physical decay processes $\rho^0 \rightarrow e^+ e^-$ and $\rho \rightarrow \pi\pi$. Certainly, a high temperature limit in which some modes vanish and others diverge

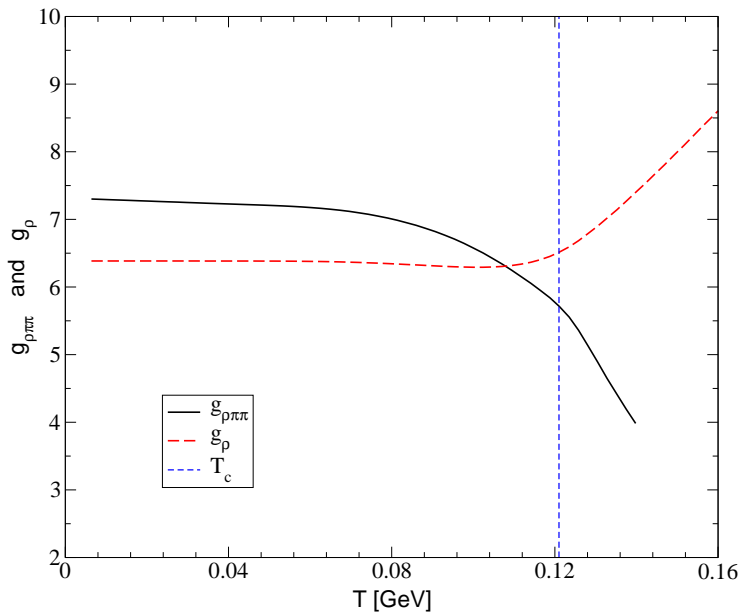


Figure 4: T -dependence of the ρ electromagnetic decay constant g_ρ (dashed line) and the strong coupling constant $g_{\rho\pi\pi}$ (solid line). Results are from the rank-2 model.

would indicate a non-analytic behavior in the reconstructed physical amplitude that is physically untenable. We therefore estimate the relevant decay widths by combining the present results for the coupling constants with the relevant phase space factors generated also from the lowest spatial mass modes.

This leads to the electromagnetic decay width

$$\Gamma_{\rho^0 \rightarrow e^+ e^-}(T) = \frac{4\pi \alpha^2 M_\rho^T(T)}{3 g_\rho(T)^2}, \quad (33)$$

while the corresponding strong decay width is

$$\Gamma_{\rho \rightarrow \pi\pi}(T) = \frac{g_{\rho\pi\pi}(T)^2 M_\rho^T(T)}{4\pi \cdot 12} \left[1 - \frac{4M_\pi(T)^2}{M_\rho^T(T)^2} \right]^{3/2}. \quad (34)$$

The T -dependence estimated in this way for the decay widths is due to the response of the quark substructure to the heat bath, particularly the restoration of chiral symmetry. The results are displayed in Fig. 5. The contrast between the behavior of the electromagnetic and strong widths near and just above T_c should be a more robust finding than the details of the individual processes. The strong width decreases rapidly and vanishes just above T_c while the electromagnetic width remains within 20% of the $T = 0$ value. Part of the strong decrease of the intrinsic $\pi\pi$ width of the transverse ρ is due to the decrease in the coupling constant, however

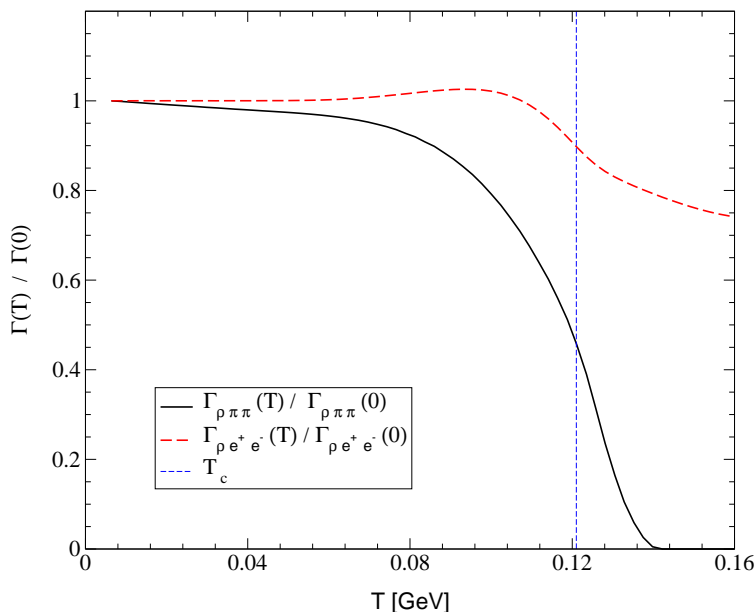


Figure 5: T -dependence of the transverse ρ partial widths due to electromagnetic e^+e^- decay (dashed line) and strong $\pi\pi$ decay (solid line) corresponding to the coupling constants shown in Fig. 4.

the dominant effect is the T -dependence of the last factor in Eq. (34). As displayed in Fig. 3, $2M_\pi(T)$ rises faster with T than does $M_\rho^T(T)$ until at $T = 1.17 T_c$ we have $M_\rho^T = 2M_\pi$. Beyond this point, the phase space factor vanishes and the strong decay $\rho^T \rightarrow \pi\pi$ is blocked. This suggests that the total ρ^T width of 151 MeV at $T = 0$ decreases by about 50% near $T = T_c$ and drops sharply to the electromagnetic value of about 6 keV by $T = 1.17 T_c$.

This narrowing of the intrinsic decay width of the vector meson mode in the heat bath is a mechanism that is distinct from the collisional broadening effect ² from the many-hadron environment. The present work indicates that there is a non-trivial T -dependence to intrinsic coupling constants such as $g_{\rho\pi\pi}$ and decay phase space. The intrinsic effect tends to significantly decrease the decay width; the many-hadron medium effects have the opposite influence. Phenomenological forms for the T -dependence of $M_\rho(T)$ and $\Gamma_{\rho^0 \rightarrow \pi\pi}(T)$ have often been explored in studies of medium effects in heavy-ion collisions. For example, both an increase in the width of the form $\Gamma_\rho^I / (1 - T^2/T_c^2)$, and a ρ mass decreasing by 50% at T_c have been explored in an effort to understand the heavy-ion dilepton spectrum ³⁴. A coordinated approach is called for in which hadronic collisional broadening mechanisms are built upon intrinsic coupling constants that respect the temperature and density dependence of the quark-gluon content.

4. Behavior at large T

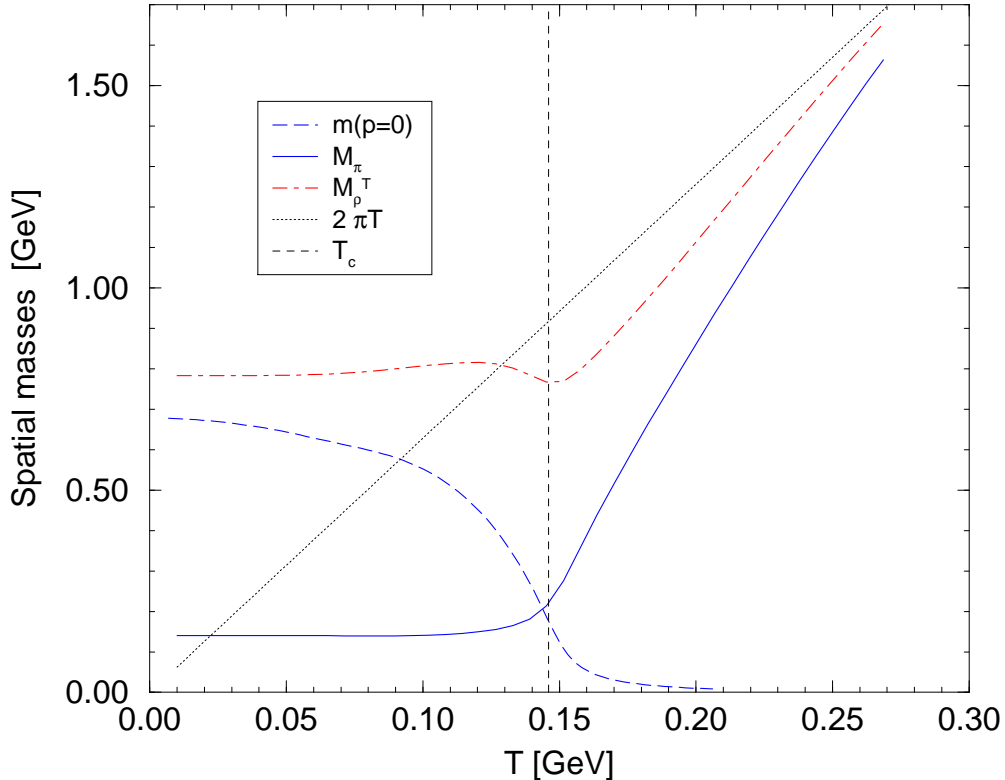


Figure 6: High T behavior of the spatial masses of the π and transverse ρ modes from the rank-1 separable model.

The quark deconfinement point T_d and the chiral restoration point T_c are generally expected to be identical or nearly so³⁵. (The present separable model produces $T_d = T_c$ in rank-1 and $T_d = 0.9 T_c$ in rank-2.) It might be expected therefore that above T_c meson modes should dissolve in favor of a gas of essentially massless quarks. However for a significant temperature range above T_c , the spatial π and ρ modes studied here continue to be stable against $\bar{q}q$ dissociation and do not dissolve into a free quark gas. This situation is clearest for the simpler rank-1 separable interaction. The results for $M_\pi(T)$ and $M_\rho^T(T)$ obtained from the eigenmass condition $\lambda(-M^2) = 1$ are displayed in Fig. 6 along with the quark dynamical mass function at $p = 0$. The masses of both spatial meson modes approach the asymptotic behavior $2\pi T$ from below. This asymptotic behavior has been discussed previously³⁶ and is observed in lattice simulations^{35,36}.

The manner in which the $2\pi T$ behavior at large T emerges from the present description is illustrated well by the rank-1 model. For $T > T_c$, the dynamically

generated mass function of the quarks is essentially negligible, and the quark propagator is dominated by the Dirac vector amplitude $\sigma_V(q_n^2) \sim 1/q_n^2$. For the spatial π mode characterized by $P = (0, \vec{P})$, the loop integral for the “polarization” function or BSE eigenvalue $\lambda_\pi(\vec{P}^2)$, given by Eq. (9), yields at large T

$$\lambda_\pi(\vec{P}^2) \approx \frac{16D_0}{3} T \int \frac{d^3q}{(2\pi)^3} f_0^2(\pi^2 T^2 + \vec{q}^2) \frac{\pi^2 T^2 + \vec{q}^2 - \frac{\vec{P}^2}{4}}{[\pi^2 T^2 + (\vec{q} + \vec{P}/2)^2][\pi^2 T^2 + (\vec{q} - \vec{P}/2)^2]}, \quad (35)$$

where only the dominant zeroth fermion Matsubara mode has been retained. For $T \gg \Lambda_0/\pi$, with Λ_0 being the range of the interaction form factor f_0 , only small q is relevant and the position of the lowest singularity as a function of $\vec{P}^2 < 0$ approaches $2\pi T$. The higher the temperature, the more $\lambda_\pi(\vec{P}^2)$ is suppressed except near the singularity. The value $\lambda_\pi(-M^2) = 1$ must be encountered before the divergence and thus $M_\pi(T) \sim 2\pi T - \Delta_\pi(T)$ where Δ_π is a positive mass defect that will typically decrease with T . Thus the spatial meson mass or screening mass will approach the thermal mass of a pair of massless fermions from below. This limit has also been demonstrated from the pseudoscalar correlator within the Nambu–Jona-Lasinio model ²⁶.

In the general case, the detailed temperature behavior of the mass defect $\Delta_\pi(T)$, or the nature of the approach to the $2\pi T$ limit, depends upon the asymptotic behavior of the quark amplitudes $A(q^2) - 1$ and $B(q^2)$. In QCD, their leading asymptotic behavior is $\sim 1/q^2$ apart from slow logarithmic corrections. The form factors chosen in this initial work within a separable model induce an exponential fall-off. It is to be expected therefore that the present model estimate of $\Delta_\pi(T)$ will decrease too rapidly with T .

In Fig. 7 the π and transverse ρ spatial masses at $T > T_c$ from both the rank-1 separable model and the ID model (see the Appendix for more details on the ID model) are presented in comparison with lattice QCD simulations of spatial screening masses ³⁶. The solid horizontal line marks 2π while the lower horizontal dot-dashed line represents the lattice free limit corrected ³⁶ for the lattice time extent N_t . From Fig. 7 it is evident that for the π at $T > T_c$, the spatial or screening mass defect $\Delta = 2\pi T - M(T)$ is decreasing more rapidly above T_c in the rank-1 separable model than is evident from the lattice simulations. This is consistent with the exponential behavior of the employed form factors. It is also consistent with the absence of quark vector self-energy amplitudes $A(p, T) - 1$ and $C(p, T) - 1$ through which interactions can be quite persistent in the asymptotic region. This can be demonstrated within the chiral limit ID model where those amplitudes are strong and indeed have the power law fall-off. As seen in Fig. 7, the resulting mass defect for both π and ρ is in fact too strong when compared with the lattice QCD simulations. This persistent self-interaction well above T_c , which slows the approach to free behavior such as Stefan-Boltzmann thermodynamics ¹⁶, may well be what is signaled by the lattice QCD data in Fig. 7.

5. Discussion

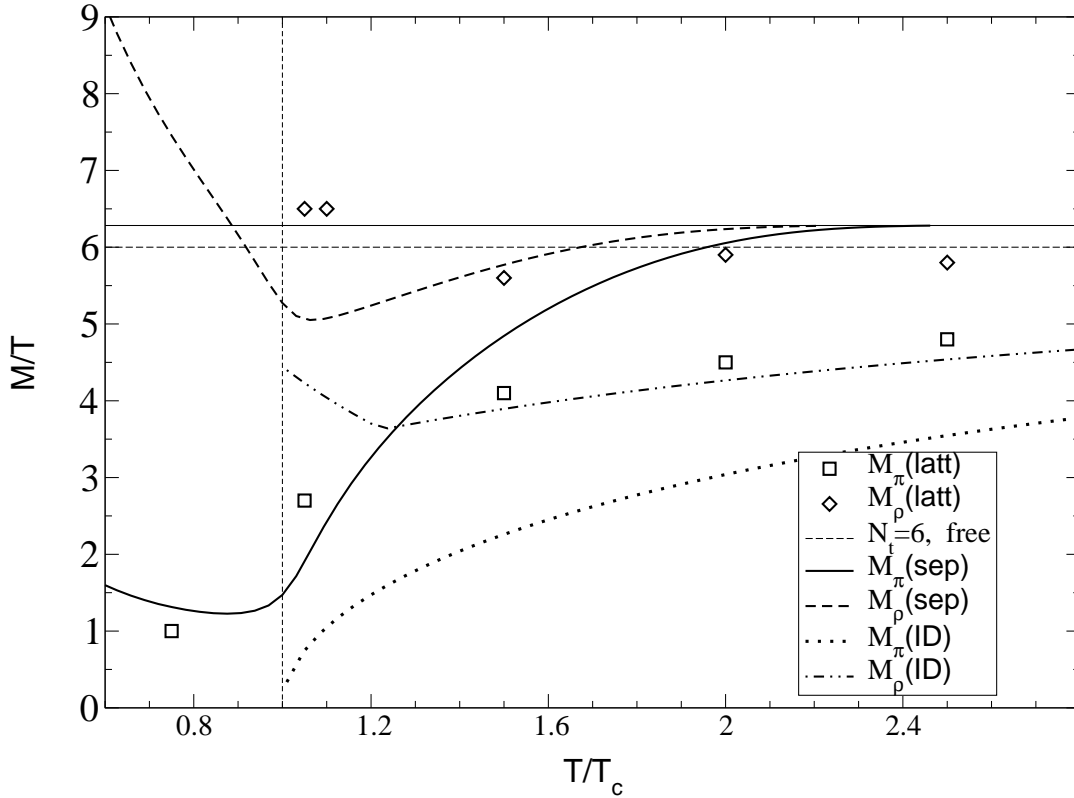


Figure 7: Spatial masses from the rank-1 separable model (sep) and the infrared-dominant model (ID) compared to spatial screening masses from lattice QCD simulations (latt) taken from ³⁶.

We have explored π and ρ spatial correlation modes at $T > 0$ within the rainbow-ladder truncation of the quark Dyson-Schwinger equation and the $\bar{q}q$ Bethe-Salpeter equation in the Matsubara formalism. With parameters fitted to $T = 0$ properties, the model possesses dynamical chiral symmetry breaking and quark confinement. A simple separable form of the effective interaction is employed and this facilitates the use of sufficient Matsubara modes to allow coverage of low temperatures as well as the transition region. Deconfinement and chiral restoration transition temperatures, T_d and T_c , are very similar and in the range 100-150 MeV. The T -evolution of the π and ρ $\bar{q}q$ states in the presence of the deconfinement and chiral restoration mechanisms is studied. The degree to which the model respects the axial vector Ward-Takahashi relation is evaluated in terms of the exact pion mass relation and the related GMOR relation. The ρ electromagnetic coupling constant g_ρ and the strong coupling constant $g_{\rho\pi\pi}$ are also obtained as a function of T . Estimates are made for the T -dependence of the widths for $\rho^0 \rightarrow e^+e^-$ and $\rho \rightarrow \pi\pi$. Finally, the high T behavior of the spatial masses is compared to that of spatial screening masses

from lattice QCD simulations³⁶.

The masses $M_\pi(T)$, $M_\rho^T(T)$ and $M_\rho^L(T)$ are found to be almost T -independent below T_c followed by a strong increase. This behavior is characteristic of lattice QCD simulations^{35,36} and DSE studies^{17,25}. Our estimate of the $\rho \rightarrow \pi\pi$ strong decay width shows a decrease with T such that, by T_c , it has been reduced by 50%. Our arguments suggest a phase-space blocking effect at about 25 MeV above T_c . (A similar phase-space blocking has been argued before only for the strong $\pi\pi$ decay of the scalar-isoscalar partner of the pion near T_c ^{24,25}.) The tendency here is for the transverse ρ mode above T_c to be left with a narrow total width typical of electromagnetic decay. One would expect the mass of the pseudoscalar K correlation to rise with T in a similar fashion to M_π , while the masses of the vector ϕ and K^* modes should rise like the ρ . This suggests that the vector modes ρ , K^* and ϕ tend to be trapped with their relatively long electroweak lifetimes and with significantly increased masses for a domain of high temperatures above the transition. Between 0.5-1.0 T_c , the transition probability connecting vector correlations with pairs of pseudoscalars would be reduced. This suggests that within the gas of pions and other pseudoscalars that dominate the hot hadronic product from heavy-ion collisions, the role of vector meson correlations in producing the dilepton spectra could be significantly less than conventional expectations. The present findings follow from the response of the quark-gluon content of the mesons to the heat bath. A different phenomenon is the coupling of the meson modes to the many-hadron environment which introduces a collisional broadening effect². An approach that incorporates both phenomena is clearly called for.

Only the spatial or screening $\bar{q}q$ masses have been investigated within this model. The temporal masses (sometimes called dynamical or pole masses) provide a different characterization of the correlations. Lattice simulations indicate that spatial masses become much larger than the temporal masses above T_c ³⁷. A Nambu–Jona-Lasinio model study²⁶ found that they are significantly different only in the range $150 \text{ MeV} < T < 350 \text{ MeV}$. A possible explanation for this discrepancy lies in our finding that the mass defect $\Delta = 2\pi T - M(T)$ at high T is significantly influenced by residual non-perturbative interaction effects in the Dirac vector amplitude $A(P^2) - 1$ of the quark self-energy. Such a term is not present in the Nambu–Jona-Lasinio model which produces a momentum-independent quark constituent mass. The present model allows low temperature confinement and a momentum-dependent quark self-energy in a simple way but at a cost of an exponential asymptotic fall-off instead of a more realistic power law fall-off. Comparison with lattice QCD results illustrates the connection between asymptotic behavior of the interaction and the high T behavior of the mass defects $\Delta_\pi(T)$ and $\Delta_\rho(T)$.

The simplicity of a separable representation of the effective quark-quark interaction of the type studied here might be of advantage in the consideration of pion loop effects and bulk thermodynamic properties of the hadron-quark matter phase transitions. Initial thermodynamic considerations have been reported recently²³. The only T -dependence of the effective quark-quark interaction implemented by

the present separable model is that generated by the Matsubara frequencies that enter through the momentum dependence. The strength and range parameters have been kept T -independent and no attempt has been made to introduce explicit T -dependent characteristics such as a Debye mass. Such considerations are more appropriately handled in approaches that have a better connection to a perturbative gluon propagator²⁵.

Acknowledgements

We acknowledge fruitful interactions and conversations with B. Van den Bossche, M. Buballa, C.D. Roberts, and S. Schmidt. The work of G.B. and Y.L.K. has been supported by the Max-Planck-Gesellschaft and by the DFG Graduiertenkolleg ‘‘Stark korrelierte Vielteilchensysteme’’. D.B. and G.B. gratefully acknowledge financial support by the Deutscher Akademischer Austauschdienst (DAAD) for visits to the Center for Nuclear Research at Kent State University where part of this work was conducted. Y.L.K. also acknowledges the Russian Fund for Fundamental Research, under contract number 97-01-01040, and the support of the Heisenberg-Landau program. P.C.T. and P.M. acknowledge support by the National Science Foundation under Grant Nos. INT-9603385 and PHY97-22429 and the hospitality of the University of Rostock where part of this work was conducted during several visits.

Appendix A

The extension to $T > 0$ of the ID model introduced at $T = 0$ by Munczek and Nemirovsky¹⁵ provides a semi-analytic perspective on the large T behavior of the meson masses. For the Feynman-like gauge used in the present study, the effective interaction of this model is specified by

$$D(p - q) \rightarrow (2\pi)^4 \frac{3\eta^2}{16} \delta^4(p - q), \quad (\text{A.1})$$

which is to be used in the DSEs given in Eqs. (4) and (5) and also in the BSE given in Eq. (1).[¶] In the chiral limit, closed form expressions exist for the resulting quark propagator amplitudes and for the ladder BSE eigenvalues $\lambda(P^2)$ in the pseudoscalar and vector channels of interest here. The chiral limit DSE solution is of the general form given in Eq. (18) with

$$\begin{aligned} \sigma_A(p^2) = \sigma_C(p^2) &= \begin{cases} \frac{2}{\eta^2}, & p^2 \leq \frac{\eta^2}{4} \\ \frac{2}{p^2} \left[1 + \left(1 + \frac{2\eta^2}{p^2} \right)^{\frac{1}{2}} \right]^{-1}, & p^2 \geq \frac{\eta^2}{4} \end{cases} \\ \sigma_B(p^2) &= \begin{cases} \frac{1}{\eta^2} (\eta^2 - 4p^2)^{\frac{1}{2}}, & p^2 \leq \frac{\eta^2}{4} \\ 0, & p^2 \geq \frac{\eta^2}{4} \end{cases}. \end{aligned} \quad (\text{A.2})$$

[¶]The results are unchanged when Landau gauge is used if Eq. (A.1) is scaled up by 4/3.

The quark mass function is $m^2(p^2) = \eta^2/4 - p^2$ for $p^2 \leq \eta^2/4$, and $m^2(p^2) = 0$ otherwise. There is no mass-shell, i.e. $p^2 + m^2(p^2) \neq 0$ for any p^2 , and there is quark confinement. The above solution holds at $T = 0$ and at $T > 0$ with p^2 replaced by $p_n^2 = \omega_n^2 + \vec{p}^2$. Thus for $T > T_c = \eta/(2\pi)$ there is chiral restoration ($\sigma_B = 0$). Results from this model at finite T, μ have been obtained for quark thermodynamics outside the phase boundary of chiral restoration as governed by the quark propagator¹⁶. The behavior of the masses of both the π and ρ modes for $T < T_c$ (and also for chemical potential dependence for $\mu < \mu_c$) have been obtained previously¹⁷.

With Eq. (A.1), the BSE given in Eq. (1) becomes

$$\lambda(P^2)\Gamma(q; P) = -\frac{\eta^2}{4}\gamma_\mu S(q_+)\Gamma(q; P)S(q_-)\gamma_\mu, \quad (\text{A.3})$$

and solutions are possible if q is fixed by P . At $T > 0$, the solution that connects smoothly to the $T = 0$ solution has the normally independent variable $q_n = (\omega_n, \vec{q})$ restricted to $q_n \rightarrow (\omega_0, \vec{0})$. To obtain spatial meson modes to compare with the separable model results, we again set $P = (0, \vec{P})$. Within the temperature domain $T < T_c = \eta/(2\pi)$, the results for the pseudoscalar and vector spatial modes are particularly simple and have been discussed previously¹⁷. One finds $\lambda_\pi(0) = 1$ for the chiral limit π ; thus $M_\pi = 0$. For the vector meson one finds that $\lambda_\rho^T(-\eta^2/2) = 1$; thus $M_\rho^T = \eta/\sqrt{2}$. These are also the correct $T = 0$ results of the model. They hold over the finite temperature domain for which the quark mass function appropriate to the propagators occurring in the BS Eq. (A.3) is nonzero. For the equation appropriate to a meson of mass M , the relevant domain for the present model is $\eta^2 - 4s > 0$ where $s = \pi^2 T^2 - M^2/4$. For $M_\pi = 0$, this temperature domain corresponds to that for which the model DSE generates a dynamical quark mass function in accord with the Goldstone theorem. For larger M , this temperature domain will be larger. The vector result $M_\rho = \eta/\sqrt{2}$ holds for the larger temperature domain $T < \sqrt{3/2}T_c$. We fix the single parameter $\eta = 1.107$ GeV, so that $M_\rho = 0.783$ GeV. This produces $T_c = 0.176$ GeV.

Beyond the temperature domain where the meson mass is constant, one finds $\lambda_\pi(\vec{P}^2) = \eta^2 s_- \sigma_A(s_+)^2$, where $s_\pm = \pi^2 T^2 \pm \vec{P}^2/4$, and the ρ eigenvalue is simply given by $\lambda_\rho^T(\vec{P}^2) = \frac{1}{2}\lambda_\pi(\vec{P}^2)$. In general both functions $\lambda(-M^2)$ decrease with increasing T and increase with increasing M . Thus the spatial eigenmode condition $\lambda(-M^2) = 1$ will tend to maintain $M_\rho^T(T) > M_\pi(T)$ while both masses rise with T , and the obtained behaviour of the masses M_ρ^T and M_π is qualitatively the same as what we found in the separable model. The main difference is that the mass defect $\Delta(T) = 2\pi T - M(T)$ is significantly larger in the ID model. The leading large T behavior

$$M_\rho^T(T)^2 \rightarrow (2\pi T)^2 \left(1 - \frac{\eta}{\pi T} \dots\right), \quad (\text{A.4})$$

leads to the spatial mass defect of the transverse ρ mode having the asymptotic value $\Delta_\rho(T) \rightarrow \eta$. Fig. 7 displays the behavior for both π and ρ .

References

- [1] *Quark Matter '99*, Eds. L. Riccati, M. Masera, and E. Vercellin, *Nucl. Phys.* **A 661** (1999).
- [2] R. Rapp and J. Wambach, “Chiral symmetry restoration and dileptons in relativistic heavy-ion collisions”, *Adv. Nucl. Phys.* in press, hep-ph/9909229; R. Rapp and C. Gale, *Phys. Rev.* **C 60**, 024903 (1999).
- [3] C. D. Roberts and A. G. Williams, *Prog. Part. Nucl. Phys.* **33**, 477 (1994); C. D. Roberts, *Fiz. Élem. Chastits At. Yadra* **30**, 537 (1999) (*Phys. Part. Nucl.* **30**, 223 (1999)).
- [4] C. D. Roberts and S. M. Schmidt, “Dyson-Schwinger Equations: Density, Temperature and Continuum Strong QCD”, *Prog. Part. Nucl. Phys.* **45**, in press (2000); nucl-th/0005064.
- [5] R. Alkofer and L. von Smekal, “The infrared behavior of QCD Green’s functions: Confinement, dynamical symmetry breaking, and hadrons as relativistic bound states,” hep-ph/0007355.
- [6] P. Maris and C. D. Roberts, *Phys. Rev.* **C 56**, 3369 (1997).
- [7] P. Maris and P. C. Tandy, *Phys. Rev.* **C 60**, 055214 (1999).
- [8] P. Maris and P. C. Tandy, *Phys. Rev.* **C 61**, 045202 (2000); P. Maris and P. C. Tandy, *Phys. Rev.* **C 62**, 055204 (2000).
- [9] P. C. Tandy, *Prog. Part. Nucl. Phys.* **39**, 117 (1997).
- [10] P. Maris and C. D. Roberts, *Phys. Rev.* **C 58**, 3659 (1998).
- [11] P. C. Tandy, *Fizika* **B 8**, 295 (1999).
- [12] M. A. Ivanov, Yu. L. Kalinovsky and C. D. Roberts, *Phys. Rev.* **D 60**, 034018 (1999).
- [13] A. Bender, D. Blaschke, Yu. L. Kalinovsky, C. D. Roberts, *Phys. Rev. Lett.* **77**, 3724 (1996) .
- [14] A. Bender, G. I. Poulis, C. D. Roberts, S. Schmidt and A. W. Thomas, *Phys. Lett.* **B 431**, 263 (1998).
- [15] H. J. Munczek and A. M. Nemirovsky, *Phys. Rev.* **D 28**, 181 (1983).
- [16] D. Blaschke, C. D. Roberts, S. Schmidt, *Phys. Lett.* **B 425**, 232 (1998).
- [17] P. Maris, C. D. Roberts, S. Schmidt, *Phys. Rev.* **C 57**, R2821 (1998).
- [18] J. C. R. Bloch, C. D. Roberts and S. M. Schmidt, *Phys. Rev.* **C 60**, 065208 (1999).
- [19] H. Ito, W. Buck and F. Gross, *Phys. Rev.* **C 43**, 2483 (1991); *Phys. Rev.* **C 45**, 1918 (1992); M. Buballa and S. Krewald, *Phys. Lett.* **B 294**, 19 (1992); R. S. Plant and M. C. Birse, *Nucl. Phys.* **A 628**, 607 (1998).
- [20] C. J. Burden, Lu Qian, C. D. Roberts, P. C. Tandy and M. J. Thomson, *Phys. Rev.* **C 55**, 2649 (1997).
- [21] S. Schmidt, D. Blaschke, and Yu. L. Kalinovsky, *Phys. Rev.* **C 50**, 435 (1994).
- [22] D. Blaschke, Yu.L. Kalinovsky and P. Tandy, in: Proc. of the XI Int. Conf. on *Problems of Quantum Field Theory*, Dubna, July 13-17, p.454, 1998; hep-ph/9811476.
- [23] D. Blaschke and P. C. Tandy, in *Understanding Deconfinement in QCD*, Eds. D. Blaschke, F. Karsch and C. D. Roberts, (World Scientific, Singapore), p. 218, 2000.
- [24] T. Hatsuda, T. Kunihiro, *Phys. Lett.* **B 185**, 304 (1987); H.A. Weldon, *Phys. Lett.* **B 274**, 133 (1992); D. Blaschke, Yu.L. Kalinovsky, S. Schmidt and H.-J. Schulze, *Phys. Rev.* **C 57**, 438 (1998); M.K. Volkov, E.A. Kuraev, D. Blaschke, G. Röpke and S. Schmidt, *Phys. Lett.* **B 424**, 235 (1998).
- [25] P. Maris, C. D. Roberts, S. M. Schmidt and P. C. Tandy, *Phys. Rev.* **C**, in press, (2000), preprint nucl-th/0001064.
- [26] W. Florkowski and B. L. Friman, *Acta. Phys. Pol.* **B 25**, 49 (1994).
- [27] C. D. Roberts, A.G. Williams and G. Krein, *Int. J. Mod. Phys.* **A 7**, 5607 (1992).
- [28] P. Maris, *Phys. Rev.* **D 52**, 6087 (1995).

- [29] P. Maris, C. D. Roberts and P. C. Tandy, *Phys. Lett.* **B 420**, 267 (1998).
- [30] L. C. L Hollenberg, C. D. Roberts and B. H. J. McKellar, *Phys. Rev.* **C 46**, 2057 (1992); D. B. Leinweber and T. D. Cohen, *Phys. Rev.* **D 49**, 3512 (1994); K. L. Mitchell and P. C. Tandy, *Phys. Rev.* **C 55**, 1477 (1995); M. A. Pichowsky, S. Walawalkar, and S. Capstick, *Phys. Rev.* **D 60**, 054030 (1999).
- [31] D. Blaschke, A. Höll, C. D. Roberts and S. Schmidt, *Phys. Rev.* **C 58**, 1758 (1998); A. Höll, P. Maris and C. D. Roberts, *Phys. Rev.* **C 59**, 1751 (1999).
- [32] N. P. Landsman and Ch. G. van Weert, *Phys. Rep.* **145**, 141 (1987).
- [33] S. Schmidt, D. Blaschke, and Yu. L. Kalinovsky, *Z. Phys.* **C 66**, 485 (1995).
- [34] H.-J. Schulze and D. Blaschke, *Phys. Lett.* **B 386**, 429 (1996).
- [35] F. Karsch and E. Laermann, *Rep. Prog. Phys.* **56**, 1347 (1993); E. Laermann, *Fiz. Élem. Chastits At. Yadra* **30**, 720 (1999) (*Phys. Part. Nucl.* **30**, 304 (1999)).
- [36] A. Gocksch, *Phys. Rev. Lett.* **67**, 1701 (1991); K. Born *et al.*, *Phys. Rev. Lett.* **67**, 302 (1991).
- [37] QCD-TARO Collaboration, "Mesons above the Deconfining transition", preprint hep-lat/9901017.